Observer-based event-triggered control in the presence of cone-bounded nonlinear inputs

L.G. Moreira, Sophie Tarbouriech, Alexandre Seuret, João Manoel Gomes da Silva

Observer-based event-triggered control in the presence of cone-bounded nonlinear inputs

L. G. Moreira[a,*], S. Tarbouriech[b], A. Seuret[b], J. M. Gomes da Silva Jr.[a]

[a] *DELAE, Universidade Federal do Rio Grande do Sul, Porto Alegre, RS, Brazil*
[b] *LAAS-CNRS, Université de Toulouse, CNRS, Toulouse, France*

Abstract

This paper presents an observer-based event-triggered strategy for linear systems subject to input cone-bounded nonlinearities. Both the emulation and co-design problems are addressed. Considering a Lyapunov approach and the cone-bound property of the input nonlinearity, sufficient conditions based on linear matrix inequalities are derived to ensure regional or global asymptotic stability of the origin of the closed-loop system. These conditions are incorporated into convex optimization problems to optimally determine the event generator parameters and the controller gain (in the co-design case) aiming at reducing the number of control updates with respect to periodic implementations for a prescribed observer gain. The event-triggering strategy considers a dwell time to cope with Zeno behaviors. Numerical examples, considering systems with quantized logarithmic inputs and saturating inputs, illustrate the potentialities of the approach.

Keywords: Event-triggered control, cone-bounded nonlinearities, observer-based control, stability, LMI.

1. Introduction

In the context of networked control systems, i.e. control systems where at least part of the communication takes place over a generic digital communication network, event-triggered control strategies have been proposed as means of dealing with communication, energy consumption and computation constraints (see, for example, [1–4] and the references therein). Considering the event-triggered control framework, there are basically two approaches. The first one is the so-called emulation design, where one considers that the controller is given *a priori* (e.g. [2, 4–7] and the references therein). In this case, the task is to synthesize an event generator that leads to a stable closed-loop system and avoids the occurrence of Zeno behavior (see, e.g. [3, 4] for an explanation of Zeno behavior). The second approach, referred in the literature as co-design, consisting in designing the control law and the event-triggering rule simultaneously, is addressed in a few papers (see [8–13]).

Many papers addressing asymptotic stability of event-triggered control systems consider state-feedback laws (e.g. [3–5, 14–17]). However, in most practical applications, only part of the system state is available or possible to be measured. Using only the available information (measured or local signals) to define the triggering mechanism and/or the control law, both for emulation and co-design approaches, is a challenging problem: see, for example, [2, 4, 7, 18–23] and [24], which also addresses the use of alternative sampling and holding functions. Moreover, most of the available literature concentrates on linear plants, even if there are a few papers dealing with generic results for nonlinear systems such as [2, 3, 6, 7].

In the recent work [25], the event-triggered control problem for the class of nonlinear systems that can be represented by a linear plant subject to cone-bounded input nonlinearities has been addressed in an emulation context. That paper considers a given observer-based feedback control law that stabilizes a

*Corresponding author
Email addresses: luciano.moreira@ufrgs.br (L. G. Moreira), tarbour@laas.fr (S. Tarbouriech), aseuret@laas.fr (A. Seuret), jmgomes@ufrgs.br (J. M. Gomes da Silva Jr.)

continuous-time implementation of the control system. The state observer allows using only local information or measurable signals in the event-triggering rule. From these assumptions, sufficient conditions in the form of linear matrix inequalities (LMIs) are proposed to ensure global asymptotic stability of the origin of the nonlinear closed-loop system under the event-triggered control strategy. These conditions are then cast into a convex optimization problem to compute the trigger parameters aiming at a reduction of the number of events, i.e. reducing the number of control updates. Addressing a similar problem, we can cite [26], which considers the absolute stabilization of event-triggered Lur'e systems in a co-design context. In that work, it is assumed that the event generator and the controller have access to the entire system state and that the nonlinearity satisfies a sector condition globally. The nonlinearity can be unknown, as long as it is ensured that it satisfies the sector condition. Also addressing the absolute stabilization of event-triggered Lur'e systems, [27] considers the emulation design and the use of only output signals in the event generator and in the controller. Only the global case is considered and a dwell time is used to avoid Zeno behavior. A variable time-delayed input approach [28] is employed to derive stability conditions in the presence of this dwell time.

In the current paper, we present a comprehensive version of our work [25] in the sense that we address also the regional stabilization and the co-design of the parameters of the event generator and the control law. We consider an approach based solely on Lyapunov methods as proposed in [3, 25, 29], without the use of the hybrid systems framework defined by [30] and used e.g. in [7, 9, 10, 12], to obtain the stability conditions. We also keep the ideas of using a dwell time to avoid Zeno behavior (see [31]) and of computing the parameters by means of solving convex optimization problems. Differently from [25], besides the extensions already mentioned, we consider a triggering function with more degrees of freedom by the use of the observed state in the event-trigger condition. In the co-design case, we consider that the observer has been previously designed and we derive conditions to simultaneously compute the state feedback matrix and the triggering function parameters. The main differences with respect to [26, 27] reside in the facts that we do not address the absolute stabilization problem, in the sense that we consider that the nonlinearity is known, we do not impose access to the entire state and we cover the co-design problem. Moreover, differently from [27], the technique employed here to cope with the dwell time does not consider a time-delay approach but an exact discretization of the closed-loop system behavior.

For both emulation and co-design cases, convex optimization problems are proposed to design the event generator parameters (and the state feedback matrix in the co-design) aiming at a reduction of the control updates (trigger activity) with respect to periodic implementations with a period equal to the dwell time chosen for the event-triggered implementation, while ensuring the regional (or global, when possible) asymptotic stability of the closed-loop system.

The present paper is organized as follows. In Section 2, the system to be considered is described as well as the problem we intend to solve. The proposed event-triggering strategy is introduced in Section 3, where suitable stability conditions in a general form are also presented. In Sections 4 and 5, stability conditions in the form of linear matrix inequalities (LMIs) along with convex optimization problems are presented to address the problem both in emulation and co-design contexts. Section 6 illustrates the potentialities of the proposed approach in the context of regional and global stabilization through two numerical examples. Finally, Section 7 presents some concluding remarks and directions for future research.

Notation. $\mathbb{N}$, $\mathbb{R}^n$ and $\mathbb{R}^{n\times m}$ denote, respectively, the sets of integers, n-dimensional vectors and $n \times m$ real matrices. For any matrix A, A' denotes its transpose. For any square matrix A, $\text{trace}(A)$ denotes its trace and $\text{He}\{A\} = A + A'$. For two symmetric matrices of the same dimensions, A and B, $A > B$ means that $A - B$ is symmetric positive definite. I and 0 stand respectively for the identity and the null matrix of appropriate dimensions. For a partitioned matrix, the symbol $*$ stands for symmetric blocks. $\lambda_{min}(A)$ and $\lambda_{max}(A)$ denote, respectively, the smallest and the largest eigenvalues of a square matrix A. $\|\cdot\|$ stands for the Euclidean norm.

2. Problem statement

Consider the following continuous-time plant:

$$\begin{cases} \dot{x}_p(t) = A_p x_p(t) + B_p u(t) + B_{pf} f(u(t)) \\ y_p(t) = C_p x_p(t) \end{cases} \tag{1}$$

where $x_p(t) \in \mathbb{R}^n$, $u(t) \in \mathbb{R}^m$, $y_p(t) \in \mathbb{R}^p$ are the state, the input and the output of the plant, respectively. Matrices A_p, B_p, B_{pf} and C_p are constant and of appropriate dimensions. Pairs (A_p, B_p) and (C_p, A_p) are supposed to be stabilizable and detectable, respectively.

Function $f : \mathbb{R}^m \to \mathbb{R}^m$ is a known, continuous, decentralized cone-bounded nonlinearity (see [32, 33], for example) affecting the input u. Therefore, it satisfies the following property:

$$f(u)'S(f(u) + Ru) \leq 0 \tag{2}$$

where $S \in \mathbb{R}^{m\times m}$ is any diagonal positive definite matrix. Matrix $R \in \mathbb{R}^{m\times m}$ is supposed to be a diagonal positive definite matrix, with diagonal elements $R_{(i,i)} \in \mathbb{R}$ defining the sector $[0, -R_{(i,i)}]$ in which the i-th component of f, i.e. $f_{(i)}$, lies. In other words, $f_{(i)}(u_{(i)})$ is supposed to satisfy $f_{(i)}(u_{(i)})(f_{(i)}(u_{(i)}) + R_{(i,i)u_{(i)}}) < 0$, $\forall i = 1, \ldots, m$. Hence, in the following, matrix R is supposed to be given according to the non-linearity function f. Property (2) can be satisfied either globally (i.e. it is valid for any $u \in \mathbb{R}^m$) or regionally (i.e. it is valid for all u in a given set $\mathcal{S}_u \subset \mathbb{R}^m$ containing the origin). In the present work, for the regional stabilization case, we consider that $\mathcal{S}_u$ is a polyhedral set, symmetric around the origin, generically defined as follows:

$$\mathcal{S}_u = \{u \in \mathbb{R}^m : |h_i' u| \leq 1;\ h_i \in \mathbb{R}^m, i = 1, ..., n_f\} \tag{3}$$

where n_f is half the number of faces. Such $f(u)$ functions can represent, for instance, nonlinearities induced by the actuators, such as dead-zones and saturations [33–35] as well as input quantization effects [25, 36, 37]. Note that depending on the case, these nonlinearities will satisfy a sector condition regionally or globally.

We consider the following observer-based feedback controller to asymptotically stabilize system (1):

$$\begin{cases} \dot{\hat{x}}(t) = A_p \hat{x}(t) + B_p u(t) + B_{pf} f(u(t)) - L e_y(t) \\ \hat{y}(t) = C_p \hat{x}(t) \\ e_y(t) = y_p(t) - \hat{y}(t) \\ u(t) = K \hat{x}(t) \end{cases} \tag{4}$$

where $\hat{x}(t) \in \mathbb{R}^n$ and $\hat{y}(t) \in \mathbb{R}^p$ are the state and the output of the observer, respectively, and $e_y(t)$ is the output error. $L \in \mathbb{R}^{n\times p}$ and $K \in \mathbb{R}^{m\times n}$ are the observer and controller gains, respectively. Note that the design of the observer assumes that the nonlinearity $f(u)$ is known. This is the case in many practical control problems, e.g. systems subject to input saturation and/or quantization.

Since we are interested in an event-triggered implementation, the control signal applied to the plant is updated only at certain instants $\{t_k\}_{k\in\mathbb{N}}$, defined by the event-triggering algorithm. The control action is held constant between two successive events by means of a zero-order-holder. Differently from classical periodic sampling techniques, the intersampling time $t_{k+1} - t_k$ is not assumed to be constant.

Thus, for all t in $[t_k\ ,\ t_{k+1})$, the closed-loop system can be represented by the following equations:

$$\begin{cases} \dot{x}_p(t) = A_p x_p(t) + B_p u(t_k) + B_{pf} f(u(t_k)) \\ \dot{\hat{x}}(t) = A_p \hat{x}(t) + B_p u(t_k) + B_{pf} f(u(t_k)) - L e_y(t) \\ u(t_k) = K \hat{x}(t_k) \\ y_p(t) = C_p x_p(t) \\ \hat{y}(t) = C_p \hat{x}(t) \\ e_y(t) = y_p(t) - \hat{y}(t) \end{cases} \tag{5}$$

In the context of a networked control implementation, system (5) represents the case in which sensors, event generator and controller are co-located, while the actuators are in a separate node of a (e.g. wireless) network. Under these circumstances, the measurement activities do not impact the network bandwidth and energy consumption as much as the control updates do. Note that for wireless networks, the sensor node can be geographically separated from the actuator node and fed by batteries. In this case, the energy consumption in data transmission is considerably higher than in the local measurement activities. Therefore, we consider the case where the outputs of the system are continuously measured.

Hence, considering system (5), we address the following problems.

Emulation design: in this case, we consider that the observer and the state feedback have been designed to ensure the asymptotic regional (or global) stability of the continuous closed-loop system. From this assumption, the goal is to devise an event-triggering strategy, i.e. to design an event-triggering function, in order to guarantee the regional (or global) asymptotic stability of the origin of the closed-loop system (5), while implicitly reducing the number of control updates (i.e. the number of events) compared to a periodic implementation with period small enough to emulate the continuous-time behavior.

Co-design: assuming that only the observer is given, the goal in this case is the joint design of the event-triggering function and the state feedback matrix to ensure the asymptotic regional (or global) stability of the closed-loop system origin and further reduce the control updates when compared to the emulation solution.

When the regional stability is concerned, the design of the event-triggered control strategy, both in emulation and co-design, should explicitly consider a given set of admissible initial conditions for which the asymptotic stability of the origin of the nonlinear closed-loop system should be ensured.

3. Event-trigger strategy

We start by providing a general formulation to the event-trigger strategy, inspired by [21, 25, 37]. Let us introduce the error vector between the value of the observed state at the last trigger instant and the current one, which is given by:

$$\delta(t) = \hat{x}(t_k) - \hat{x}(t) \tag{6}$$

and the following generic rule to determine the event instants:

$$t_{k+1} = \min\{t \geq t_k + T, \quad s.t. \quad g(\delta(t), y_a(t)) \geq 0\} \tag{7}$$

where y_a represents the vector of available information to the event generator, which corresponds, in our case, to $y_a(t) = \begin{bmatrix}\hat{x}(t)' & e_y(t)'\end{bmatrix}'$, and T is the (minimum) dwell time, during which the function g is not evaluated and thus the control action is not updated. Note that we are implicitly assuming in the definition of $y_a(t)$ that $y_p(t)$ is continuously measured, i.e. it is available at each $t \geq 0$. The function $g : \mathbb{R}^n \times \mathbb{R}^{n+p} \to \mathbb{R}$ and the dwell time $T > 0$ have to be efficiently defined such that the asymptotic stability of the origin of the closed-loop system (5) under the event-triggering rule described in (7) is ensured. Typically, the dwell time T is chosen as small as allowed by the network and computational constraints of the system. In this case, the event-triggering mechanism is responsible for delaying the occurrence of control updates, reducing its number with respect to a periodic implementation, whose sampling period is equal to the dwell time chosen. Observe also that the triggering condition considers $g(\delta(t), y_a(t)) \geq 0$ instead of the more usual test criterion $g(\delta(t), y_a(t)) = 0$ (as in [3]). This is because when a dwell time T is considered, $g(\delta(t), y_a(t))$ is not evaluated during the interval $t \in [t_k, t_k + T)$. Therefore, it can become greater than zero in this interval and thus stay greater than zero when it is evaluated, at the instant $t_k + T$.

Note that rule (7) ensures a minimum inter-event time of T, which prevents Zeno behavior. It also uses only available information since $\delta(t)$ only depends on the observed state $\hat{x}(t)$, its sampled value at the instant t_k and the system output (recall that $e_y(t) = y_p(t) - C\hat{x}(t)$).

At this point, it is convenient to re-write system (5) in terms of the observer state $\hat{x}(t)$ and the observer error $e(t) = x_p(t) - \hat{x}(t)$. Considering this change of variables and the definition of $\delta(t)$ in (6), the closed-loop

system can be represented as follows:

$$\begin{cases} \dot{\hat{x}}(t) = (A_p + B_pK)\hat{x}(t) + B_pK\delta(t) + B_{pf}f(u(t_k)) - LC_pe(t) \\ \dot{e}(t) = (A_p + LC_p)e(t). \end{cases} \tag{8}$$

Defining the augmented state vector

$$x(t) \;=\; \begin{bmatrix} \hat{x}(t)' & e(t)' \end{bmatrix}' \in \mathbb{R}^{2n} \tag{9}$$

and matrices

$$A_a = \begin{bmatrix} A_p & -LC_p \\ 0 & A_p + LC_p \end{bmatrix}, \qquad B_a = \begin{bmatrix} B_p \\ 0 \end{bmatrix}, \qquad B_{af} = \begin{bmatrix} B_{pf} \\ 0 \end{bmatrix}, \qquad C_a = \begin{bmatrix} I & 0 \\ 0 & C_p \end{bmatrix}, \tag{10}$$

system (8) can be rewritten as:

$$\dot{x}(t) = \left(A_a + B_a \begin{bmatrix} K & 0 \end{bmatrix}\right) x(t) + B_aK\delta(t) + B_{af}f(u(t_k)). \tag{11}$$

Then the following general theorem provides sufficient conditions for the regional asymptotic stability of the origin of (11), or, equivalently, of (5).

Theorem 1. *Consider system* (11) *with* $x(t) \in \mathbb{R}^{2n}$ *as defined in* (9) *and* $f(u)$ *satisfying* (2), $\forall u \in \mathcal{S}_u$, *with* $\mathcal{S}_u$ *defined in* (3). *Consider also a scalar* $T > 0$, *a function* $g : \mathbb{R}^n \times \mathbb{R}^{n+p} \to \mathbb{R}$ *and the triggering rule given by* (7). *If there exist a function* $V : \mathbb{R}^{2n} \to \mathbb{R}$, *diagonal positive definite matrices* $S_1 \in \mathbb{R}^{m\times m}$, $S_2 \in \mathbb{R}^{m\times m}$ *and positive scalars* ϵ_1, ϵ_2 *and* ϵ_3 *such that the following relations are verified:*

(i) $\epsilon_1||x||^2 \leq V(x) \leq \epsilon_2||x||^2$

(ii) $\dot{V}(x(t)) - g(\delta(t), y_a(t)) - 2f(u(t_k))'S_1(f(u(t_k)) + Ru(t_k)) < 0, \forall t \in [t_k + T \;,\; t_{k+1}),\ \forall k \in \mathbb{N},\ x(t) \neq 0$

(iii) $V(x(t_k + T)) - V(x(t_k)) - 2f(u(t_k))'S_2(f(u(t_k)) + Ru(t_k)) < -\epsilon_3\|x(t_k)\|^2, \qquad \forall k \in \mathbb{N},\ x(t_k) \neq 0$

(iv) $V(x(t_k)) - u(t_k)'h_ih_i'u(t_k) > 0, \qquad \forall k \in \mathbb{N},\ i = 1, ..., n_f$

then, the origin of system (11) *with the triggering rule* (7) *is regionally asymptotically stable, the set* $\mathcal{L}_v = \{x \in \mathbb{R}^{2n} : V(x) \leq 1\}$ *is included in the region of attraction of the origin and the inter-event intervals are lower bounded by* T.

Proof. The stability analysis is carried out considering the time intervals $[t_k \;,\; t_k + T)$ and $[t_k + T,\; t_{k+1})$. Let us first analyze the interval $[t_k \;,\; t_k + T)$. From (*iii*) and property (2), the function $V(x)$ satisfies

$$V(x(t_k + T)) < V(x(t_k)) - \epsilon_3\|x(t_k)\|^2 \tag{12}$$

as long as $u(t_k) \in \mathcal{S}_u$.

Moreover, from (11), the definition of δ and the fact that $u(t_k) = \begin{bmatrix} K & 0 \end{bmatrix} x(t_k)$, it follows that

$$\dot{x}(t) = A_ax(t) + B_au(t_k) + B_{af}f(u(t_k)) \tag{13}$$

and thus

$$x(t_k + \tau) = e^{A_a\tau}x(t_k) + \int_{t_k}^{t_k+\tau} e^{A_a(t_k+\tau-s)}ds\big(B_au(t_k) + B_{af}f(u(t_k))\big). \tag{14}$$

Taking into account that $\|f(v)\| \leq \gamma\|v\|$ for any vector $v \in \mathcal{S}_u$, where γ is a positive constant depending on the norm of matrix R, one obtains that

$$\|x(t_k + \tau)\| \leq \left(\|e^{A_a\tau}\| + \left\|\int_{t_k}^{t_k+\tau} e^{A_a(t_k+\tau-s)}ds\right\| (\|B_a\| + \gamma\|B_{af}\|) \left\|\begin{bmatrix} K & 0 \end{bmatrix}\right\|\right) \|x(t_k)\| \tag{15}$$

and thus, since the trajectories of (11) are continuous, there exists $\beta > 0$ such that

$$\|x(t_k + \tau)\| \leq \beta \|x(t_k)\| \qquad \forall \tau \in [0, T]. \tag{16}$$

This means that during the dwell time T, i.e. for $t \in [t_k, t_k + T]$, the trajectories of the system are uniformly bounded, provided that $u(t_k) \in \mathcal{S}_u$. Therefore, during the dwell time T, the Lyapunov function is not necessarily strictly decreasing. From (i) and (16) we can only ensure that its value is bounded $\forall \tau \in [0, T]$ and, from (12), that $V(x(t_k + T)) < V(x(t_k))$.

Consider now the interval $[t_k + T,\ t_{k+1})$. If (ii) is satisfied, then we have:

$$\dot{V}(x(t)) < g(\delta(t), y_a(t)) + 2f(u(t_k))' S_1 (f(u(t_k)) + Ru(t_k)) \tag{17}$$

and it follows from (2) and (7) that $g(\delta(t), y_a(t)) + 2f(u(t_k))' S_1 (f(u(t_k)) + Ru(t_k)) \leq 0$. We conclude that condition (ii) implies that $\dot{V}(x(t)) < 0$ in the interval $[t_k + T,\ t_{k+1})$ and therefore

$$V(x(t)) < V(x(t_k + T)), \quad \forall t \in [t_k + T,\ t_{k+1}),\ \forall k \in \mathbb{N} \tag{18}$$

provided that $u(t_k) \in \mathcal{S}_u$.

Hence, from (12) and (18), we conclude that

$$V(x(t_{k+1})) < V(x(t_k)) - \epsilon_3 \|x(t_k)\|^2 \tag{19}$$

provided that $u(t_k) \in \mathcal{S}_u$.

Now, recalling that $u(t_k) \in \mathcal{S}_u \iff |h_i' u(t_k)| \leq 1;\ i = 1, ..., n_f$, the satisfaction of (iv) actually ensures that $u(t_k) \in \mathcal{S}_u$ as long as $x(t_k) \in \mathcal{L}_v$. This in conjunction with (19) implies that $x(t_k) \in \mathcal{L}_v$ and therefore $u(t_k) \in \mathcal{S}_u,\ \forall k \in \mathbb{N}$, provided that $x(t_0) = x(0) \in \mathcal{L}_v$. From (19), it follows that $\lim_{k\to\infty} V(x(t_k)) = 0$. Hence, from (i), we have $\|x(t_k)\|^2 \leq \epsilon_1^{-1} V(x(t_k))$ and it follows that $\lim_{k\to\infty} x(t_k) = 0$, provided that $x(0) \in \mathcal{L}_v$. This fact, along with (16), ensures that $\lim_{t\to\infty} x(t) = 0$, which means that system (11) is asymptotically stable and $\mathcal{L}_v$ is included in its region of attraction.

In addition, note that T is a lower bound on the inter-sampling times by using Lemma 1 in [21], preventing Zeno behavior. □

It should be noticed that the conditions of Theorem 1 are implicitly locally verified due to statement (iv). In fact, (ii) and (iii) should be verified only if $x(t_k)$ and $u(t_k)$ satisfy (iv). Assuming that $u(t_k) = \begin{bmatrix} K & 0 \end{bmatrix} x(t_k)$, this means the conditions are verified only if $x(t_k)$ belongs to the level set $\mathcal{L}_v$ of the function V, which is included in the set $\mathcal{S}_x = \{x \in \mathbb{R}^{2n} : \left|h_i' \begin{bmatrix} K & 0 \end{bmatrix} x\right| \leq 1,\ i = 1, ..., n_f\}$.

In the global case (i.e. when relation (2) is satisfied $\forall u \in \mathbb{R}^m$), one retrieves Theorem 1 of [25], in which case relation (iv) is no longer necessary. This is recalled here in the following corollary.

Corollary 1. *Consider a scalar $T > 0$, a function $g : \mathbb{R}^n \times \mathbb{R}^{n+p} \to \mathbb{R}$ and the triggering rule given by* (7)*. Assume that the property* (2) *is globally satisfied and the conditions (i), (ii) and (iii) of Theorem 1 are verified. Then, the origin of system* (11) *with the triggering rule* (7) *is globally asymptotically stable and the inter-event intervals are lower bounded by T.*

Proof. The proof mimics that of Theorem 1 without the need of using the constraint (iv) since property (2) is globally satisfied, i.e. it is valid $\forall u(t_k) \in \mathbb{R}^m$. □

Remark 1. *Notice that satisfaction of conditions (i), (iii) and (iv) of Theorem 1 ensures that a periodic implementation of the control system with period T is asymptotically stable in the regional case. In the global case, satisfaction of (i) and (iii) are enough to ensure asymptotic stability since property* (2) *is globally satisfied.*

4. Emulation case

In this section, Theorem 1 is considered to extend the emulation design method presented in [25] to the regional stabilization case. In other words, we want to propose a way to design the event-triggering rule using only the available signals (i.e. $\hat{x}(t)$ and $e_y(t)$), when the controller and observer gains, K and L respectively, are given *a priori* and the nonlinearity f satisfies property (2) regionally. Results for the global case are presented as a corollary.

We consider a triggering function similar to the one proposed in [25], i.e. $g(\delta(t), y_a(t))$ defined as follows:

$$g(\delta(t), y_a(t)) = \delta(t)' Q_\delta \delta(t) - \begin{bmatrix} \hat{x}(t) \\ e_y(t) \end{bmatrix}' Q_\epsilon^{-1} \begin{bmatrix} \hat{x}(t) \\ e_y(t) \end{bmatrix}. \tag{20}$$

It should be noticed that, differently from [25], $\delta(t)$ does not depend on K here. Hence, the following theorem establishes conditions for the regional asymptotic stability of system (11) under the event-triggered control strategy given in (7).

Theorem 2. *Consider $f(u)$ verifying (2) for all $u \in \mathcal{S}_u$, with $\mathcal{S}_u$ as defined in (3). Given controller and observer gains K and L and a scalar $T > 0$, if there exist symmetric positive definite matrices $\bar{Q}_\delta$, Q_ϵ, $W = \left[\begin{smallmatrix} W_1 & W_2 \\ * & W_3 \end{smallmatrix}\right]$ and diagonal positive definite matrices U_1 and U_2 of appropriate dimensions such that the following LMIs*

$$\Phi_1 = \begin{bmatrix} M_1 & \begin{bmatrix} WC_a' \\ 0 \\ 0 \end{bmatrix} \\ * & -Q_\epsilon \end{bmatrix} < 0 \tag{21}$$

$$\Phi_2 = \begin{bmatrix} -W & -W \begin{bmatrix} K' \\ 0 \end{bmatrix} R & W \left(A_{ad}(T)' + \begin{bmatrix} K' \\ 0 \end{bmatrix} B_a' B_{ad}(T)' \right) \\ * & -2U_2 & U_2 B_{af}' B_{ad}(T)' \\ * & * & -W \end{bmatrix} < 0 \tag{22}$$

$$\Phi_3 = \begin{bmatrix} W & W \begin{bmatrix} K' \\ 0 \end{bmatrix} h_i \\ * & 1 \end{bmatrix} > 0 \qquad i = 1, ..., n_f \tag{23}$$

are verified with A_a, B_a, B_{af}, C_a as defined in (10) and

$$\begin{aligned} M_1 = \mathrm{He} \left\{ \begin{bmatrix} I \\ 0 \\ 0 \end{bmatrix} \begin{bmatrix} (A_a + B_a \begin{bmatrix} K & 0 \end{bmatrix}) W & B_a K W_1 & B_{af} U_1 \end{bmatrix} \right\} - \begin{bmatrix} 0 \\ I \\ 0 \end{bmatrix} \bar{Q}_\delta \begin{bmatrix} 0 & I & 0 \end{bmatrix} \\ - \mathrm{He} \left\{ \begin{bmatrix} 0 \\ 0 \\ I \end{bmatrix} \begin{bmatrix} R \begin{bmatrix} K & 0 \end{bmatrix} W & RKW_1 & U_1 \end{bmatrix} \right\}, \end{aligned} \tag{24}$$

$$A_{ad}(T) = e^{A_a T}, \qquad B_{ad}(T) = \int_0^T e^{A_a s} ds,$$

then, the event-triggering rule (7) with g as defined in (20) and $Q_\delta = W_1^{-1} \bar{Q}_\delta W_1^{-1}$ is such that the origin of system (11) is regionally asymptotically stable and the set $\mathcal{L}_v = \left\{ x \in \mathbb{R}^{2n} : x' W^{-1} x \leq 1 \right\}$, is included in its region of attraction. Furthermore, the inter-sampling times are lower bounded by T.

Proof. Consider the quadratic Lyapunov candidate function for system (11) given by

$$V(x(t)) = x(t)' W^{-1} x(t), \tag{25}$$

where the matrix W^{-1} is positive definite thanks to the satisfaction of (22) and (23), implying that condition (i) of Theorem 1 is satisfied. We show next that the LMIs (21)–(23) are sufficient conditions for inequalities (ii)–(iv) of Theorem 1 to hold.

Considering the time-derivative of V along the trajectories of system (11) for any $t \in [t_k + T,\ t_{k+1})$, the following expression is obtained:

$$\begin{aligned}\Psi_c(t) &:= \dot{V}(x(t)) - \delta(t)'Q_\delta\delta(t) + \begin{bmatrix}\hat{x}(t)\\ e_y(t)\end{bmatrix}' Q_\epsilon^{-1}\begin{bmatrix}\hat{x}(t)\\ e_y(t)\end{bmatrix} - 2f(u(t_k))'S_1(f(u(t_k)) + Ru(t_k)) \\ &= \begin{bmatrix} x(t)\\ \delta(t)\\ f(u(t_k))\end{bmatrix}' \Gamma \begin{bmatrix} x(t)\\ \delta(t)\\ f(u(t_k))\end{bmatrix},\end{aligned}$$

with

$$\begin{aligned}\Gamma = \mathrm{He}\left\{\begin{bmatrix}I\\0\\0\end{bmatrix} W^{-1}\begin{bmatrix}\left(A_a + B_a\begin{bmatrix}K & 0\end{bmatrix}\right) & B_aK & B_{af}\end{bmatrix}\right\} - \begin{bmatrix}0\\I\\0\end{bmatrix} Q_\delta \begin{bmatrix}0 & I & 0\end{bmatrix} + \begin{bmatrix}C_a'\\0\\0\end{bmatrix} Q_\epsilon^{-1}\begin{bmatrix}C_a & 0 & 0\end{bmatrix} \\ - \mathrm{He}\left\{\begin{bmatrix}0\\0\\I\end{bmatrix}\begin{bmatrix}S_1R\begin{bmatrix}K & 0\end{bmatrix} & S_1RK & S_1\end{bmatrix}\right\},\end{aligned}$$

where we used the facts that $u(t_k) = K\hat{x}(t_k) = K\hat{x}(t) + K\delta(t)$ and $e_y(t) = C_pe(t)$ for the last equality.

Hence, imposing $\Gamma < 0$ guarantees that $\Psi_c(t) < 0$. Now, pre- and post-multiplying Γ by $\mathrm{diag}(W, W_1, U_1)$ with $U_1 = S_1^{-1}$, making the change of variables $\bar{Q}_\delta = W_1Q_\delta W_1$ and considering the Schur complement, it follows that inequality $\Phi_1 < 0$ in (21) implies $\Gamma < 0$ and, therefore, $\Psi_c(t) < 0$. This also implies that condition (ii) of Theorem 1 is verified when considering $g\left(\delta(t), \begin{bmatrix}\hat{x}(t)' & e_y(t)'\end{bmatrix}'\right)$ as defined in (20) with $Q_\delta = W_1^{-1}\bar{Q}_\delta W_1^{-1}$.

Now pre- and post-multiplying (23) by $\mathrm{diag}(W^{-1}, 1)$ and applying the Schur complement, one obtains:

$$W^{-1} - \begin{bmatrix}K'h_i\\0\end{bmatrix}\begin{bmatrix}h_i'K & 0\end{bmatrix} > 0. \tag{26}$$

Pre- and post-multiplying (26) by $x(t_k)'$ and $x(t_k)$, respectively, the satisfaction of (23) implies that the following condition is fulfilled:

$$x(t_k)'W^{-1}x(t_k) - \hat{x}(t_k)'K'h_ih_i'K\hat{x}(t_k) > 0. \tag{27}$$

Thus, recalling the definition of $V(x)$ in (25) and that $u(t_k) = K\hat{x}(t_k)$, the satisfaction of (27) (or, equivalently, (23)) implies that condition (iv) of Theorem 1 is verified.

Now, in order to prove that condition (iii) of Theorem 1 holds if (22) is satisfied, note that solving the linear differential equation (11) over the interval $[t_k,\ t_k + T]$ yields

$$x(t_k + T) = \Lambda_1(T)x(t_k) + \Lambda_2(T)f(u(t_k)) \tag{28}$$

where

$$\Lambda_1(T) \triangleq A_{ad}(T) + B_{ad}(T)B_a\begin{bmatrix}K & 0\end{bmatrix}, \quad \Lambda_2(T) \triangleq B_{ad}(T)B_{af}.$$

with $A_{ad}(T)$ and $B_{ad}(T)$ as defined in (24).

Hence, from (28), condition (iii) in Theorem 1 can be written as

$$\begin{aligned}\Psi_T(t_k) &:= \Delta V_T(x) - 2f(u(t_k))'S_2(f(u(t_k)) + Ru(t_k)) \\ &= \Big(\Lambda_1(T)x(t_k) + \Lambda_2(T)f(u(t_k))\Big)' W^{-1}\Big(\Lambda_1(T)x(t_k) + \Lambda_2(T)f(u(t_k))\Big) - x(t_k)'W^{-1}x(t_k) \\ &\quad - 2f(u(t_k))'S_2\Big(f(u(t_k)) + Ru(t_k)\Big) < -\epsilon_3\|x(t_k)\|\end{aligned}$$

with $\Delta V_T(x) = V(x(t_k+T)) - V(x(t_k))$. Applying the Schur complement and a congruence transformation with $\mathrm{diag}(W, U_2, W)$, where $U_2 = S_2^{-1}$, it can be seen that condition $\Phi_2 < 0$ in (22) ensures that there exists $\epsilon_3 > 0$ such that condition (iii) in Theorem 1 is satisfied. The proof is then concluded by invoking Theorem 1. We can conclude that the solutions to system (11) converge asymptotically to the origin if they start in $\mathcal{L}_v$. Furthermore, the event-triggering strategy defined by (7) and (20) implicitly ensures that the inter-event times are lower bounded by T. □

The following corollary addresses the global case in an emulation design context.

Corollary 2. *Consider $f(u)$ verifying (2) $\forall u \in \mathbb{R}^m$. Given controller and observer gains K and L and a scalar $T > 0$, if there exist symmetric positive definite matrices $\bar{Q}_\delta$, Q_ϵ and $W = \left[\begin{smallmatrix} W_1 & W_2 \\ * & W_3 \end{smallmatrix}\right]$ and diagonal positive definite matrices U_1 and U_2 of appropriate dimensions such that LMIs (21) and (22) are verified, then the event-triggered sampling rule (7) with (20) and $Q_\delta = W_1^{-1}\bar{Q}_\delta W_1^{-1}$ is such that the origin of system (11) is globally asymptotically stable. Furthermore, the inter-sampling times are lower bounded by T.*

Proof. The proof mimics that of Theorem 2 without the need of using constraint (23) since property (2) is globally satisfied. □

4.1. Tuning – Emulation case

Conditions in Theorem 2 are LMIs, provided that K, L and T are fixed, corresponding to the emulation problem. The gains K and L can be designed, for instance, disregarding the input nonlinearity, by classical methods of linear control or by applying more sophisticated nonlinear techniques based on sector bound conditions for continuous-time systems (see, for instance [33]). In this case, the conditions in Theorem 2 allow assessing the stability under an aperiodic sampled-data control law driven by the event-triggering strategy while taking explicitly into account the system input nonlinearity.

Let us point out that differently from [21], in Theorem 2 the inter-event times are directly obtained via the satisfaction of (22) without the need of additional *a posteriori* calculations. Furthermore, if conditions (21) and (23) hold, it is always possible to find a small enough T such that the set of conditions (21), (22) and (23) is verified. Then, T appears as a tuning parameter of the event-triggered problem. If T is too large, the conditions may be unfeasible. Since a large T can lead to a performance degradation with respect to the continuous-time implementation, a classical trade-off has to be considered when choosing T.

Hence, assuming previously determined gains K and L and an appropriately chosen T, the idea is to optimally compute matrices Q_ϵ and Q_δ, aiming at postponing the events with respect to the dwell time T, thus reducing the control updates when compared to a periodic implementation with period T, while ensuring the closed-loop stability in a given set $\mathcal{X}_0$ of admissible initial conditions. With this goal, we can consider $\mathcal{X}_0$ as an ellipsoidal set described as follows:

$$\mathcal{X}_0 = \left\{ x \in \mathbb{R}^{2n} : x' P_0 x \leq 1 \right\}, \tag{29}$$

where P_0 is a given symmetric positive definite matrix. Then the selection of the triggering function parameters can be systematically performed through the following convex optimization problem:

$$\begin{aligned} \min_{W, \bar{Q}_\delta, Q_\epsilon, U_1, U_2} \quad & \mathrm{trace}(\bar{Q}_\delta) + \mathrm{trace}(Q_\epsilon) \\ \text{subject to (21), (22), (23), } & W > P_0^{-1}. \end{aligned} \tag{30}$$

The motivation behind the optimization criterion in (30) is to get $\bar{Q}_\delta$ and Q_ϵ as "small" as possible. From the definition of the triggering function (20) and the fact that $\bar{Q}_\delta = W_1 Q_\delta W_1$, this optimization means that matrix $Q_\delta > 0$ is implicitly minimized by minimizing $\bar{Q}_\delta > 0$ while matrix $Q_\epsilon^{-1} > 0$ is maximized. Since an event is generated and the control input is updated only when the function g is positive, this optimization procedure aims at reducing the impact of the first positive contribution in g ($Q_\delta > 0$) over the second negative contribution ($-Q_\epsilon < 0$). In other words, it implicitly implies more time before a new event occurs. Inequality $W > P_0^{-1}$ ensures $\mathcal{X}_0 \subset \mathcal{L}_v$, guaranteeing that all trajectories starting in $\mathcal{X}_0$ converge asymptotically to the origin.

For the case of global stabilization, one uses the conditions of Corollary 2 and there is no need to ensure $\mathcal{X}_0 \subset \mathcal{L}_v$. Hence, optimization problem (30), without (23) and $W > P_0^{-1}$, can be considered.

Remark 2. *Considering the parameters K, L, Q_δ, Q_ϵ and T given, Theorem 2 can also be used to provide an estimate of the region of attraction of the origin of the closed-loop system under the triggered control law.*

In this case, one needs to pre- and post-multiply Φ_1 by $\mathrm{diag}(I, W_1^{-1}, I)$ in order to get Q_δ explicitly (instead of $\bar{Q}_\delta$) in the LMI, which leads to:

$$\begin{bmatrix} M_2 & \begin{bmatrix} WC_a' \\ 0 \\ 0 \end{bmatrix} \\ * & -Q_\epsilon \end{bmatrix} < 0, \tag{31}$$

with

$$M_2 = \mathrm{He}\left\{ \begin{bmatrix} I \\ 0 \\ 0 \end{bmatrix} \begin{bmatrix} (A_a + B_a \begin{bmatrix} K & 0 \end{bmatrix})W & B_a K & B_{af} U_1 \end{bmatrix} \right\} - \begin{bmatrix} 0 \\ I \\ 0 \end{bmatrix} Q_\delta \begin{bmatrix} 0 & I & 0 \end{bmatrix} - \mathrm{He}\left\{ \begin{bmatrix} 0 \\ 0 \\ I \end{bmatrix} \begin{bmatrix} R \begin{bmatrix} K & 0 \end{bmatrix} W & RK & U_1 \end{bmatrix} \right\}.$$

Then it suffices to define and solve a new optimization problem where the objective function maximizes the set $\mathcal{L}_v$ in some sense (e.g. maximizing the trace of W, maximizing the lowest eigenvalue of W, etc). For instance, we can consider:

$$\begin{aligned} &\max_{W, U_1, U_2} \ \mathrm{trace}(W) \\ &\quad \textit{subject to } (22),\ (23),\ (31). \end{aligned} \tag{32}$$

5. Co-design

In this section, we address the co-design problem stated in Section 2. The idea here is to jointly design the matrix K and the event-triggering function parameters, i.e. matrices Q_ϵ and Q_δ, for a given observer gain L. Hence, taking as a starting point the emulation design, the problem can therefore be seen as re-computing the gain K in order to further reduce the trigger activity or possibly to enlarge the region of stability.

It is worth noticing that, if K, Q_ϵ and $\bar{Q}_\delta$ are free variables, the conditions in Theorem 2 are no longer LMIs. To obtain tractable LMI stabilization conditions, one solution is to impose some additional constraints on the structure of matrix W. This is formalized in the next theorem.

Theorem 3. *Consider $f(u)$ verifying (2) for all $u \in \mathcal{S}_u$, with $\mathcal{S}_u$ as defined in (3). Given an observer gain matrix L and a scalar $T > 0$, assume there exist symmetric positive definite matrices $\bar{Q}_\delta$, Q_ϵ, $W = \left[\begin{smallmatrix} W_1 & 0 \\ 0 & W_3 \end{smallmatrix}\right]$, diagonal positive definite matrices U_1 and U_2 and a matrix Y_1 of appropriate dimensions such that the following LMIs are satisfied:*

$$\Omega_1 = \begin{bmatrix} M_3 & \begin{bmatrix} WC_a' \\ 0 \\ 0 \end{bmatrix} \\ * & -Q_\epsilon \end{bmatrix} < 0, \tag{33}$$

$$\Omega_2 = \begin{bmatrix} -W & -\begin{bmatrix} Y_1' \\ 0 \end{bmatrix} R & WA_{ad}(T)' + \begin{bmatrix} Y_1' \\ 0 \end{bmatrix} B_a' B_{ad}(T)' \\ * & -2U_2 & U_2 B_{af}' B_{ad}(T)' \\ * & * & -W \end{bmatrix} < 0, \tag{34}$$

$$\Omega_3 = \begin{bmatrix} W & \begin{bmatrix} Y_1' \\ 0 \end{bmatrix} h_i \\ * & 1 \end{bmatrix} > 0, \tag{35}$$

with

$$M_3 = \mathrm{He}\left\{ \begin{bmatrix} I \\ 0 \\ 0 \end{bmatrix} \begin{bmatrix} A_a W + B_a \begin{bmatrix} Y_1 & 0 \end{bmatrix} & B_a Y_1 & B_{af} U_1 \end{bmatrix} \right\} - \begin{bmatrix} 0 \\ I \\ 0 \end{bmatrix} \bar{Q}_\delta \begin{bmatrix} 0 & I & 0 \end{bmatrix}$$
$$- \mathrm{He}\left\{ \begin{bmatrix} 0 \\ 0 \\ I \end{bmatrix} \begin{bmatrix} R \begin{bmatrix} Y_1 & 0 \end{bmatrix} & RY_1 & U_1 \end{bmatrix} \right\},$$

and the matrices A_a, B_a, B_{af}, C_a, $A_{ad}(T)$, $B_{ad}(T)$ as defined in (10) *and in* (24)*. Then, the event-triggered sampling rule defined by* (7) *and* (20) *with $Q_\delta = W_1^{-1} \bar{Q}_\delta W_1^{-1}$ is such that the origin of system* (11) *with $K = Y_1 W_1^{-1}$ is regionally asymptotically stable and the set $\mathcal{L}_v = \left\{ x \in \mathbb{R}^{2n} : x' W^{-1} x \leq 1 \right\}$ is included in its region of attraction. Furthermore, the inter-sampling times are lower bounded by T.*

Proof. The proof follows the same steps taken in the proof of Theorem 2 except that we impose the following structure to matrix $W = \left[\begin{smallmatrix} W_1 & 0 \\ 0 & W_3 \end{smallmatrix} \right]$, implying that $\begin{bmatrix} K & 0 \end{bmatrix} W = \begin{bmatrix} KW_1 & 0 \end{bmatrix}$ and then the change of variables $Y_1 = KW_1$ is done to linearize the conditions. □

The following corollary addresses the global case in the co-design context.

Corollary 3. *Consider $f(u)$ verifying* (2) *$\forall u \in \mathbb{R}^m$. Given an observer gain matrix L and a scalar $T > 0$, assume there exist symmetric positive definite matrices $\bar{Q}_\delta$, Q_ϵ, $W = \left[\begin{smallmatrix} W_1 & 0 \\ 0 & W_3 \end{smallmatrix} \right]$, diagonal positive definite matrices U_1 and U_2 and a matrix Y_1 of appropriate dimensions such that the LMIs* (33) *and* (34) *are satisfied. Then, the event-triggered sampling rule defined by* (7) *and* (20) *with $Q_\delta = W_1^{-1} \bar{Q}_\delta W_1^{-1}$ is such that the origin of system* (11) *with $K = Y_1 W_1^{-1}$ is globally asymptotically stable. Furthermore, the inter-sampling times are lower bounded by T.*

Proof. It mimics the proof of Theorem 3 without the need of constraint (35) because property (2) is globally satisfied. □

5.1. Tuning – Co-design

Conditions in Theorem 3 are LMIs provided L and T are fixed. The parameters of the triggering function Q_δ, Q_ϵ and the controller gain matrix K are simultaneously computed by solving the following convex optimization problem:

$$\begin{aligned} \min_{W, Y_1, \bar{Q}_\delta, Q_\epsilon, U_1, U_2} \quad & \mathrm{trace}(\bar{Q}_\delta) + \mathrm{trace}(Q_\epsilon) \\ \text{subject to } & (33),\ (34),\ (35),\ W > P_0^{-1}. \end{aligned} \tag{36}$$

The reasoning behind the optimization problem (36) is the same as the one behind (30).

In the case of global stabilization, i.e. when the relation (2) is satisfied $\forall u \in \mathbb{R}^m$, the conditions of Corollary 3 should be used. In this case, the optimization problem (36) without conditions (35) and $W > P_0^{-1}$ should be considered.

Remark 3. *The emulation design employs conditions that are less conservative than the co-design, as it uses an unconstrained (i.e., without an imposed structure) Lyapunov matrix W. Thus, after solving the co-design optimization problem* (36) *to obtain a new suitable gain K, one can use this value of K as an input to the emulation optimization problem* (30)*, aiming at a further reduction in the number of events while guaranteeing that the given set of initial conditions can be stabilized. The process, referred as co-design refinement, is illustrated in Section 6. It is worth noticing that once K is obtained from the co-design problem* (36)*, the solution obtained is also a feasible solution of the emulation problem* (30)*. In this case, the value of the objective function, in terms of matrices $\bar{Q}_\delta$ and Q_ϵ, will always be less than or equal to the one obtained in the co-design problem, leading to a potential reduction in the number of generated events. Although this events reduction cannot be formally guaranteed, this is quite likely to happen, as illustrated in the numerical examples.*

Remark 4. *The simultaneous design of Q_δ, Q_ϵ, K, L and T is a challenging co-design problem. Unfortunately, if one considers L as a decision variable, it is not possible to linearize the conditions of Theorem 3. Note that, due to the method used to integrate the trajectories of the system in the interval $[t_k, t_k + T]$, L and T appear as part of exponential terms. On the other hand, it should be noticed that the simultaneous synthesis of the control and observer gains considering the augmented system and a quadratic Lyapunov function is a non-convex problem even when continuous-time controllers and linear systems are considered. Hence, it remains an open problem not only in the event-triggered control context.*

6. Numerical examples

6.1. Example 1 – Regional stabilization

System data:

Let us consider the following plant:

$$\begin{cases} \dot{x}_p(t) = \begin{bmatrix} 0 & 1 \\ 4 & 0 \end{bmatrix} x_p(t) + \begin{bmatrix} 0 \\ 1 \end{bmatrix} q(u(t)) \\ y_p(t) = \begin{bmatrix} 1 & 0 \end{bmatrix} x_p(t) \end{cases} \tag{37}$$

where $q(u)$ is a logarithmic quantization function defined as follows [36]:

$$q(u) = \begin{cases} \mu_q & \text{if} \quad u \geq \frac{\mu_q}{1+\delta_q} \\ \rho_q^j \mu_q & \text{if} \quad \frac{\rho_q^j \mu_q}{1+\delta_q} \leq u < \frac{\rho_q^j \mu_q}{1-\delta_q},\ j \in \{1, 2, ...\} \\ 0 & \text{if} \quad u = 0 \\ -\rho_q^j \mu_q & \text{if} \quad -\frac{\rho_q^j \mu_q}{1+\delta_q} \geq u > -\frac{\rho_q^j \mu_q}{1-\delta_q},\ j \in \{1, 2, ...\} \\ -\mu_q & \text{if} \quad u \leq -\frac{\mu_q}{1+\delta_q} \end{cases}$$

with the quantization parameters:

$$0 < \rho_q < 1, \qquad \delta_q = \frac{1-\rho_q}{1+\rho_q}, \qquad \mu_q > 0.$$

ρ_q specifies the density of quantization and μ_q defines the maximum absolute level of quantization, which can be seen as an implicit saturation of the control signal. Figure 1 shows a graphical representation of the positive branch of this logarithmic quantization function.

It should be noticed that the quantization error $\tilde{q}(u) = q(u) - u$ is regionally restricted to the cone defined by $\pm\delta_q u$ (i.e. it satisfies the relation $(\tilde{q}(u) - \delta_q u)(\tilde{q}(u) + \delta_q u) \leq 0$) for all values of u satisfying $|u| \leq \frac{\mu_q}{1-\delta_q}$ (see [38]). In order to cast the system in the form (1), with a function $f(u)$ satisfying (2), it suffices to consider:

$$f(u) = \tilde{q}(u) - \delta_q u, \quad A_p = \begin{bmatrix} 0 & 1 \\ 4 & 0 \end{bmatrix}, \quad B_{pf} = \begin{bmatrix} 0 \\ 1 \end{bmatrix}, \quad B_p = (1+\delta_q) B_{pf}, \quad C_p = \begin{bmatrix} 1 & 0 \end{bmatrix}.$$

Note that in this case the relation $(\tilde{q}(u) + \delta_q u)(\tilde{q}(u) - \delta_q u) \leq 0$ becomes $f(u)(f(u) + 2\delta_q u) \leq 0$, i.e. (2) is verified with $R = 2\delta_q$. Moreover, this relation is satisfied as long as $|u| \leq \frac{\mu_q}{1-\delta_q}$, that is, $\left| \frac{1-\delta_q}{\mu_q} u \right| \leq 1$, i.e. $h_1 = \frac{1-\delta_q}{\mu_q}$ in (3).

We consider the quantization with $\rho_q = 0.9$ (which leads to $R = 2\delta_q = 0.105263$) and $\mu_q = 35$.

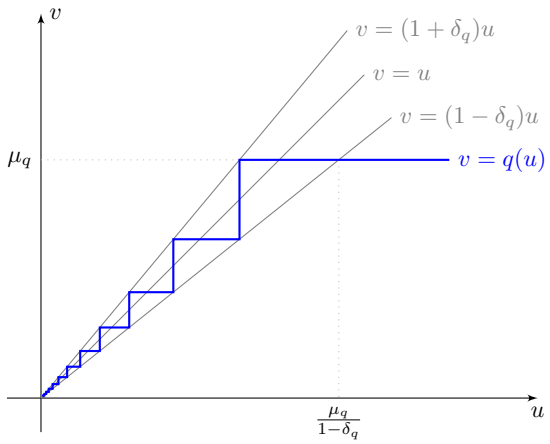

Figure 1: Logarithmic quantization function (positive branch).

Optimization results:

Considering the feedback gain matrix $K = \begin{bmatrix} -4.8 & -1.9 \end{bmatrix}$, the observer gain matrix $L = \begin{bmatrix} -3.5 & -7 \end{bmatrix}'$, $\mathcal{X}_0$ defined as in (29) with $P_0 = \text{diag}(10^6, 10^6, 0.1, 0.1)$ and the dwell time $T = 0.02$, we solve the emulation design optimization problem (30) with additional conditions $\lambda_{min}(Q_\delta) > 10^{-4}$ and $\lambda_{max}(Q_\epsilon) < 10^3 \lambda_{min}(Q_\epsilon)$ to prevent Q_δ and Q_ϵ from becoming ill-conditioned, obtaining the following results:

$$Q_\epsilon = \begin{bmatrix} 848.8 & 188.2 & 98.71 \\ 188.2 & 101.4 & 18.31 \\ 98.71 & 18.31 & 27.89 \end{bmatrix}, \quad Q_\delta = \begin{bmatrix} 1.162 & 0.4599 \\ 0.4599 & 0.1822 \end{bmatrix}.$$

Using the same values $L = \begin{bmatrix} -3.5 & -7 \end{bmatrix}'$, $P_0 = \text{diag}(10^6, 10^6, 0.1, 0.1)$ and $T = 0.02$, the co-design optimization problem (36) with the same additional conditions to prevent Q_δ and Q_ϵ from becoming ill-conditioned yields:

$$K = \begin{bmatrix} -9.299 & -4.598 \end{bmatrix}, \quad Q_\epsilon = \begin{bmatrix} 201.9 & -7.784 & 122.3 \\ -7.784 & 44.37 & 11.15 \\ 122.3 & 11.15 & 81.26 \end{bmatrix}, \quad Q_\delta = \begin{bmatrix} 4.309 & 2.131 \\ 2.131 & 1.054 \end{bmatrix}.$$

As mentioned in Remark 3, we can refine these results by solving the emulation optimization problem (30) with the gain $K = \begin{bmatrix} -9.299 & -4.598 \end{bmatrix}$ obtained in the co-design. This yields the following matrices for the triggering function:

$$Q_\epsilon = \begin{bmatrix} 63.14 & 1.518 & 37.73 \\ 1.518 & 52.2 & 25.8 \\ 37.73 & 25.8 & 36.2 \end{bmatrix}, \qquad Q_\delta = \begin{bmatrix} 1.929 & 0.9537 \\ 0.9537 & 0.4716 \end{bmatrix}.$$

The ellipses defined by the intersection between the plane $\hat{x} = 0$ and the sets $\mathcal{L}_v = \{x \in \mathbb{R}^{2n} : x'W^{-1}x \leq 1\}$ for each W obtained with the optimization problems above are shown in Figure 2 (in dashed red line), along with the intersection between the same plane and the border of $\mathcal{X}_0$ (in solid black lines). This figure also depicts phase portraits of the systems, with blue circle marks showing initial conditions for which the trajectories converge to the origin and magenta plus signs showing initial conditions that lead to divergent trajectories. One can see that, in all cases, the ellipses contain $\mathcal{X}_0$, as required by the optimization problems. It is also visible that the sets $\mathcal{L}_v$ are contained in the region of attraction of the origin in each case and, therefore, can be used as estimates for it.

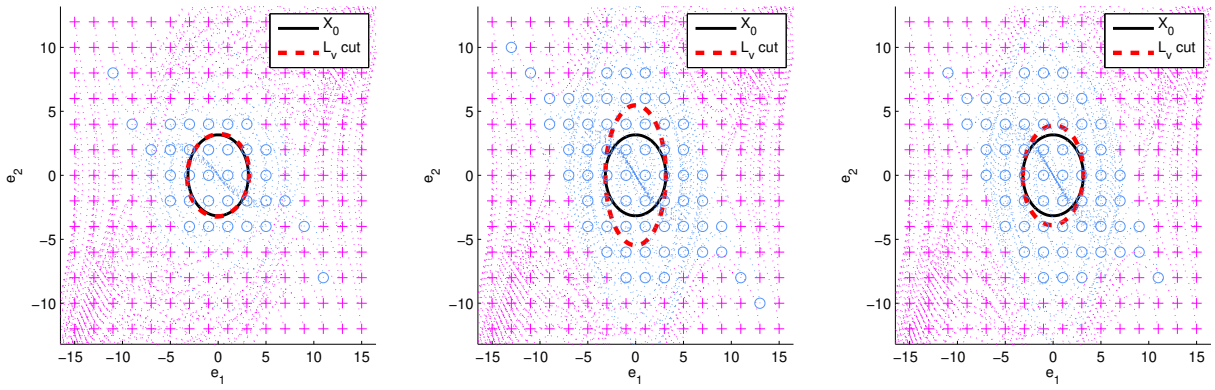

a) Emulation b) Co-design c) Co-design refinement

Figure 2: Example 1 – Phase portraits, $\mathcal{L}_v$ and $\mathcal{X}_0$ sets

Table 1: Example 1 – Average number of control updates for 100 different initial conditions

T	Emulation	Co-design	Co-design refinement	Periodic
0.01	65.56	50.33	35.00	1000
0.02	65.47	50.13	34.47	500
0.03	65.67	48.48	34.72	333.3
0.04	65.05	43.48	32.45	250
0.043	64.60	40.38	30.86	232.6
0.044	64.09	40.55	29.64	227.3
0.045	64.24	unfeasible	–	222.2
0.05	63.31	unfeasible	–	200
0.10	64.25	unfeasible	–	100
0.11	unfeasible	unfeasible	–	–

Influence of T:

Table 1 shows the influence of T in the results. It depicts the average number of control updates for simulations within the time interval $[0, 10]$ considering 100 different initial plant states, distributed along the boundary of the respective $\mathcal{L}_v$ set, for various values of T, for each of the proposed design methods and for a periodic controller [1] with period T. The initial state of the observer is set as zero in all simulations. One can see that T has an expressive impact on the number of events generated in the co-design and refinement cases, but not in the emulation case. In the emulation context, the impact of T is highly dependent on the system characteristics and the chosen value of K. Different behaviors can occur for different choices of K. Moreover, notice that the co-design problem is not feasible for some values of T where the emulation problem is. This can be expected since the co-design conditions are more restrictive than the emulation ones due to the structure imposed to W. It is also shown that the co-design problem leads to less events and that the refinement procedure described in Remark 3 reduces even more their number. A comparison with the periodic controllers considering a period T (i.e., equals to the dwell time) shows that all the event-triggered controllers resulted in less control updates.

Simulations:

Here we present simulations of the closed-loop systems designed from optimization problems (30) and (36) and also with the co-design refinements proposed in Remark 3, considering two different values of T.

[1] For the periodic controller, the numbers of events are exact and independent of the initial conditions.

In all simulations, the initial conditions for the plant and the observer are, respectively:

$$x_p(0) = \begin{bmatrix} -3 \\ 0 \end{bmatrix}, \quad \hat{x}(0) = \begin{bmatrix} 0 \\ 0 \end{bmatrix}.$$

Figures 3 and 4 depict the plant and observer states in the top plots. It can be noticed that the observer states converge to the plant states, as expected, and also the convergence of the plant states to the origin. The middle plots show the control action. Note that it is indeed held constant between two events. Moreover, the value of the control is subject to a logarithmic quantization. The bottom plot depicts the event instants, with the sizes of the bars representing the inter-event times, i.e. the difference between the time of that event and the previous one. It can be seen that the trigger strategy effectively delays the event instants, yielding inter-event times larger than the dwell time while ensuring the asymptotic stability of the closed-loop system. The figures also highlight that the co-design and refinement processes result in less events than the emulation. The figures depict the simulation for t in the interval $[0, 10]$. If we extend the simulation time, no appreciable changes occur: Inter-event times keep similar to the pattern shown just before $t = 10$ and the trajectories continue to converge to the origin. It should be pointed out that matrix A_p is unstable in the example at hand.

6.2. Example 2 – Global stabilization

System data:

Here we consider the following stable plant:

$$\begin{cases} \dot{x}_p(t) = \begin{bmatrix} -1 & 2 \\ -2 & 0 \end{bmatrix} x_p(t) + \begin{bmatrix} 0 \\ 1 \end{bmatrix} \text{sat}(u(t)) \\ y_p(t) = \begin{bmatrix} 1 & 0 \end{bmatrix} x_p(t) \end{cases} \tag{38}$$

where $\text{sat}(\cdot)$ is a saturation function with saturation levels at ± 5. Note that (38) can be re-written in the form (1) with $B_p = \begin{bmatrix} 0 \\ 1 \end{bmatrix}$ by assuming $f(u) = sat(u) - u$ to be a dead-zone function, which satisfies condition (2) with $R = 1$ globally, i.e. $\forall u \in \mathbb{R}^m$. Moreover, since A_p in this case is Hurwitz, the global stabilization under saturating inputs can be achieved [39].

Optimization results:

Consider first the emulation case with $K = \begin{bmatrix} 2 & -4 \end{bmatrix}$ and $L = \begin{bmatrix} -20 & -53 \end{bmatrix}'$. In this case, the eigenvalues of $A_p + B_pK$ are -1 and -4 and the eigenvalues of $A_p + LC_p$ are -10 and -11. Choosing a dwell time $T = 0.1$, and solving the version of optimization problem (30) suitable for the global case (i.e. with conditions given by Corollary 2), with modifications to impose a minimum exponential decay rate of 0.75 so that the closed-loop solution does not degenerate into the open-loop one, i.e. imposing $\dot{V}(x(t)) < -0.75V(x(t))$ and $V(x(t_k + T)) - V(x(t_k)) < (e^{-0.75T} - 1)V(x(t_k))$, one obtains the following results:

$$Q_\epsilon = \begin{bmatrix} 3.581 & 0.5562 & -0.001386 \\ 0.5562 & 2.715 & 0.008729 \\ -0.001386 & 0.008729 & 0.7225 \end{bmatrix}, \quad Q_\delta = \begin{bmatrix} 9.922 & -9.883 \\ -9.883 & 17.38 \end{bmatrix}.$$

For the co-design case, considering the same values of $L = \begin{bmatrix} -20 & -53 \end{bmatrix}'$, $T = 0.1$ and the same additional conditions related to the conditioning of matrices and exponential decay rate, the solution to the version of optimization problem (36) suitable for the global case leads to:

$$K = \begin{bmatrix} 1.232 & -4.6503 \end{bmatrix}, \quad Q_\epsilon = \begin{bmatrix} 1.067 & 0.1554 & 0.0005847 \\ 0.1554 & 1.058 & 0.002162 \\ 0.0005847 & 0.002162 & 0.1619 \end{bmatrix}, \quad Q_\delta = \begin{bmatrix} 6.266 & -5.72 \\ -5.72 & 16.92 \end{bmatrix}.$$

Table 2: Example 2 – Average number of control updates for 100 different initial conditions

T	Emulation	Co-design	Co-design refinement	Periodic
0.01	78.58	53.82	49.23	1000
0.05	73.50	48.88	46.35	200
0.10	60.18	48.74	45.15	100
0.20	50.00	50.00	50.00	50
0.30	34.00	34.00	34.00	33.33
0.40	25.00	25.00	25.00	25
0.50	unfeasible	20.00	20.00	20
0.60	unfeasible	17.00	17.00	16.67

Refining the event-triggering function as mentioned in Remark 3, one obtains:

$$Q_\epsilon = \begin{bmatrix} 0.3437 & 0.04672 & 0.0003135 \\ 0.04672 & 0.3302 & 0.001317 \\ 0.0003135 & 0.001317 & 0.06555 \end{bmatrix}, \quad Q_\delta = \begin{bmatrix} 15.98 & -15.15 \\ -15.15 & 43.56 \end{bmatrix}.$$

Influence of T:

Table 2 shows the influence of T in the results. It depicts the average number of control updates for simulations considering 100 different initial plant states distributed along the unit circle and within the time interval $[0, 10]$ for various values of T, for each of the proposed design methods and for a periodic controller with period T. The initial state of the observer is set as zero in all simulations. One can see that, for small values of T, the co-design leads again to less events and that the refinements mentioned in Remark 3 allow to further reduce the number of events. Also, the event-triggered controllers generate less events than the periodic ones. On the other hand, for larger values of T, all three methods give the same results. As it is going to be shown in the simulations, this is because, in the present example, when T increases, the event-triggering mechanism becomes less effective and the triggering becomes periodic with period T. Table 2 also shows that, for this system and the particular value of K considered in the emulation design, the co-design allows choosing a wider range of values for the dwell time T. This illustrates again that, in the emulation case, the impact of T is highly dependent on the system characteristics and the chosen value of K. In the example at hand, with the chosen $K = \begin{bmatrix} 2 & -4 \end{bmatrix}$, a periodic controller with a period greater than 0.5 leads to a closed-loop system that is not asymptotically stable. That explains why the emulation problem becomes unfeasible for $T \geq 0.5$. On the other hand, the co-design problem (which computes a different K) and the co-design refinement (which uses K from the corresponding co-design) are still feasible for $T = 0.5$ and $T = 0.6$.

Simulations:

In this section, we present simulations of the closed-loop systems from an emulation and a co-design point of view for two different values of T. We also include simulations of the systems obtained with the refinements proposed in Remark 3. In all simulations, the initial conditions for the plant and the observer are, respectively:

$$x_p(0) = \begin{bmatrix} -12 \\ 5 \end{bmatrix}, \quad \hat{x}(0) = \begin{bmatrix} 0 \\ 0 \end{bmatrix}.$$

Figures 5 and 6 depict the plant and observer states in the top plots. The observer states quickly converge to the plant states and the state converges to the origin, as expected. The middle plots show the control action, where one can note that it indeed saturates at the values ± 5. The bottom plot depicts the event instants, with the sizes of the bars representing the inter-event times. One can see that the triggering strategy effectively delays the event instants for low values of T; but when T increases, the event-triggering mechanism becomes less effective and the triggering becomes periodic.

7. Conclusion

In this paper we have addressed the design of observer-based event-triggered control for a class of nonlinear systems formed by a linear plant subject to input cone-bounded nonlinearities. Emulation design and co-design of the event generator parameters and the controller gain have been addressed both for regional and global stabilization cases. The proposed techniques use only the measurable outputs. An observer is used to recover the plant state variables that are not available. Sufficient conditions in the form of LMIs associated to convex optimization problems have been proposed to co-design the feedback gain (K) and event-trigger parameters (Q_δ, Q_ϵ) to ensure the regional (or global when possible) asymptotic stability of the closed-loop system while aiming at reducing the number of events with respect to periodic implementations. The approach allows to design the event-triggering rule with a parameter T imposing a minimum inter-event time, which prevents the Zeno behavior occurrence. Numerical examples illustrated the application of the methodology and highlighted the superiority of results achievable in the co-design context with respect to the number of events generated.

The co-design of Q_δ, Q_ϵ, K, L and T is still an open problem and is subject of ongoing work. Approaches considering sampled-data systems instead of the exact discretization can be of value to avoid the exponential terms on T and L, thus allowing the partial co-design case where L, Q_δ and Q_ϵ are the decision variables.

The extension of the methods to address noise and event-triggered measurements are also interesting topics for future work. These are challenging topics due to the more complex observation error dynamics that arises when handling these situations.

8. Acknowledgements

This study was financed in part by the Coordenação de Aperfeiçoamento de Pessoal de Nível Superior - Brazil (CAPES) - Finance Code 001 (PROEX, PDSE 88881.134305/2016-01, SticAmSud 88881.143275/2017-01); CNPq, Brazil (grants PQ-305979/2015-9 and Univ-422992/2016-0).

[1] R. Postoyan, A. Girard, Triggering mechanism using freely selected sensors for linear time-invariant systems, in: 54th IEEE Conference on Decision and Control, Osaka, Japan, 2015, pp. 4812–4817.

[2] R. Postoyan, P. Tabuada, D. Nešić, A. Anta, A framework for the event-triggered stabilization of nonlinear systems, IEEE Trans. Autom. Control 60 (4) (2015) 982–996.

[3] P. Tabuada, Event-triggered real-time scheduling of stabilizing control tasks, IEEE Trans. Autom. Control 52 (9) (2007) 1680–1685.

[4] W. Heemels, K. Johansson, P. Tabuada, An introduction to event-triggered and self-triggered control, in: 51st IEEE Conference on Decision and Control, Maui, HI, USA, 2012, pp. 3270–3285.

[5] X. Wang, M. Lemmon, Event design in event-triggered feedback control systems, in: 47th IEEE Conference on Decision and Control, Cancun, Mexico, 2008, pp. 2105–2110.

[6] A. Seuret, C. Prieur, Event-triggered sampling algorithms based on a Lyapunov function, in: 50th IEEE Conference on Decision and Control and European Control Conference, Orlando, Florida, 2011, pp. 6128–6133.

[7] M. Abdelrahim, R. Postoyan, J. Daafouz, D. Nešić, Stabilization of nonlinear systems using event-triggered output feedback controllers, IEEE Trans. Autom. Control 61 (9) (2016) 2682–2687.

[8] K. Aström, Event based control, in: Analysis and design of nonlinear control systems, Springer-Verlag, Berlin Heidelberg, 2008, pp. 127–147.

[9] A. Seuret, C. Prieur, S. Tarbouriech, L. Zaccarian, Event-triggered sampling for linear closed-loop systems with plant input saturation, in: 9th IFAC Symposium on Nonlinear Control Systems, Toulouse, France, 2013, pp. 341–346.

[10] A. Seuret, C. Prieur, S. Tarbouriech, L. Zaccarian, LQ-based event-triggered controller co-design for saturated linear systems, Automatica 74 (2016) 47–54.

[11] W.-P.-M.-H. Heemels, M.-C.-F. Donkers, A.-R. Teel, Periodic event-triggered control for linear systems, IEEE Trans. Autom. Control 58 (4) (2013) 847–861.

[12] M. Abdelrahim, R. Postoyan, J. Daafouz, D. Nešić, Co-design of output feedback laws and event-triggering conditions for linear systems, in: 53rd IEEE Conference on Decision and Control, Los Angeles, CA, USA, 2014, pp. 3560–3565.

[13] D. Antunes, W.-P.-M.-H. Heemels, P. Tabuada, Dynamic programming formulation of periodic event-triggered control: Performance guarantees and co-design., in: 51th IEEE Conference on Decision and Control, Maui, HI, USA, 2012, pp. 7212–7217.

[14] D. Lehmann, J. Lunze, Extension and experimental evaluation of an event-based state-feedback approach, Control Engineering Practice 19 (2) (2011) 101–112.

[15] W. Wu, S. Reimann, S. Liu, Event-triggered control for linear systems subject to actuator saturation, IFAC Proceedings Volumes 47 (3) (2014) 9492 – 9497, 19th IFAC World Congress.

[16] E. Aranda-Escolastico, M. Guinaldo, S. Dormido, A novel approach for periodic event-triggering based on general quadratic functions, in: 2015 International Conference on Event-based Control, Communication, and Signal Processing (EBCCSP), Krakow, Poland, 2015, pp. 1–6.
[17] L. G. Moreira, L. B. Groff, J. M. Gomes da Silva Jr., Event-triggered state-feedback control for continuous-time plants subject to input saturation, Journal of Control, Automation and Electrical Systems 27 (5) (2016) 473–484.
[18] D. Lehmann, J. Lunze, Event-based output feedback control, in: 19th IEEE Mediterranean Conference on Control and Automation, Corfu, Greece, 2011, pp. 982–987.
[19] J. Almeida, C. Silvestre, A.-M. Pascoal, Observer based self-triggered control of linear plants with unknown disturbances, in: American Control Conference, Montreal, Canada, 2012, pp. 5688–5693.
[20] M. C. F. Donkers, W. P. M. H. Heemels, Output-based event-triggered control with guaranteed $\mathcal{L}_\infty$-gain and improved and decentralized event-triggering, IEEE Trans. Autom. Control 57 (6) (2012) 1362–1376.
[21] P. Tallapragada, N. Chopra, Event-triggered dynamic output feedback control for LTI systems, in: 51st IEEE Conference on Decision and Control, Maui, HI, USA, 2012, pp. 6597–6602.
[22] X. Wang, M.-D. Lemmon, Event-triggering in distributed networked control systems, IEEE Trans. Autom. Control 56 (3) (2011) 586–601.
[23] C. Xia, H. Fei, Observer based event-triggered control for certain and uncertain linear systems, IMA Journal of Mathematics Control and Information 30 (4) (2013) 1–16.
[24] M. Braksmayer, L. Mirkin, $\mathcal{H}_2$ optimization under intermittent sampling and its application to event-triggered control, IFAC-PapersOnLine 50 (1) (2017) 7869–7874, 20th IFAC World Congress.
[25] S. Tarbouriech, A. Seuret, L. G. Moreira, J. M. Gomes da Silva Jr., Observer-based event-triggered control for linear systems subject to cone-bounded nonlinearities, IFAC-PapersOnLine 50 (1) (2017) 7893–7898, 20th IFAC World Congress.
[26] F. Zhang, M. Mazo, N. van de Wouw, Absolute stabilization of Lur'e systems under event-triggered feedback, IFAC-PapersOnLine 50 (1) (2017) 15301 – 15306, 20th IFAC World Congress.
[27] R. E. Seifullaev, A. L. Fradkov, Event-triggered control of sampled-data nonlinear systems, IFAC-PapersOnLine 49 (14) (2016) 12 – 17, 6th IFAC Workshop on Periodic Control Systems PSYCO 2016.
[28] E. Fridman, A. Seuret, J.-P. Richard, Robust sampled-data stabilization of linear systems: an input delay approach, Automatica 40 (8) (2004) 1441 – 1446.
[29] S. Tarbouriech, A. Seuret, J. M. Gomes da Silva Jr., D. Sbarbaro, Observer-based event-triggered control co-design for linear systems, IET Control Theory & Applications 10 (18) (2016) 2466–2473.
[30] R. Goebel, R. Sanfelice, A. R. Teel, Hybrid Dynamical Systems: Modeling, Stability, and Robustness, Princeton University Press, 2012.
[31] M. Mazo, A. Anta, P. Tabuada, An ISS self-triggered implementation of linear controllers, Automatica 46 (8) (2010) 1310–1314.
[32] H. K. Khalil, Nonlinear systems, 2nd Edition, Prentice Hall, Upper Saddle River, (N.J.), 1996.
[33] E.-B. Castelan, S. Tarbouriech, I. Queinnec, Control design for a class of nonlinear continuous-time systems, Automatica 44 (8) (2008) 2034–2039.
[34] S. Tarbouriech, G. Garcia, J. M. Gomes da Silva Jr., I. Queinnec, Stability and Stabilization of Linear Systems with Saturating Actuators, Springer, 2011.
[35] L. Zaccarian, A.-R. Teel, Modern anti-windup synthesis, Princeton University Press, 2011.
[36] M. Fu, L. Xie, The sector bound approach to quantized feedback control, IEEE Trans. Autom. Control 50 (11) (2005) 1698–1711.
[37] P. Tallapragada, N. Chopra, On event triggered tracking for nonlinear systems, IEEE Trans. Autom. Control 58 (9) (2013) 2343–2348.
[38] C. de Souza, D. Coutinho, M. Fu, Stability analysis of finite-level quantized discrete-time linear control systems, European Journal of Control 16 (3) (2010) 258–271.
[39] H. J. Sussmann, E. D. Sontag, Y. Yang, A general result on the stabilization of linear systems using bounded controls, IEEE Trans. Autom. Control 39 (12) (1994) 2411–2425.

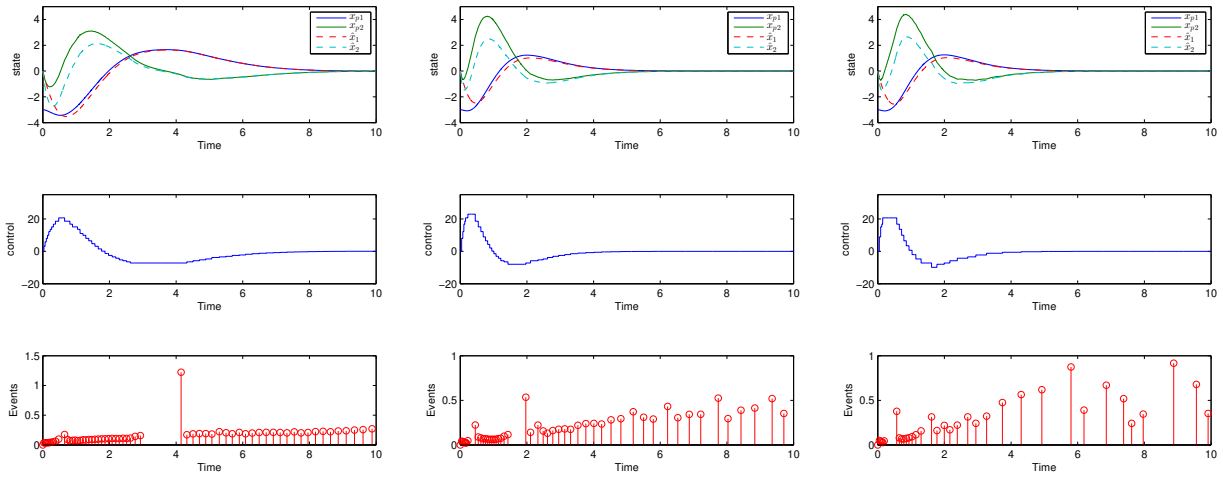

a) Emulation b) Co-design c) Co-design refinement

Figure 3: Example 1 – Evolution of the state of the plant and the observer, the control input u, and the sampling instants. $T = 0.02$

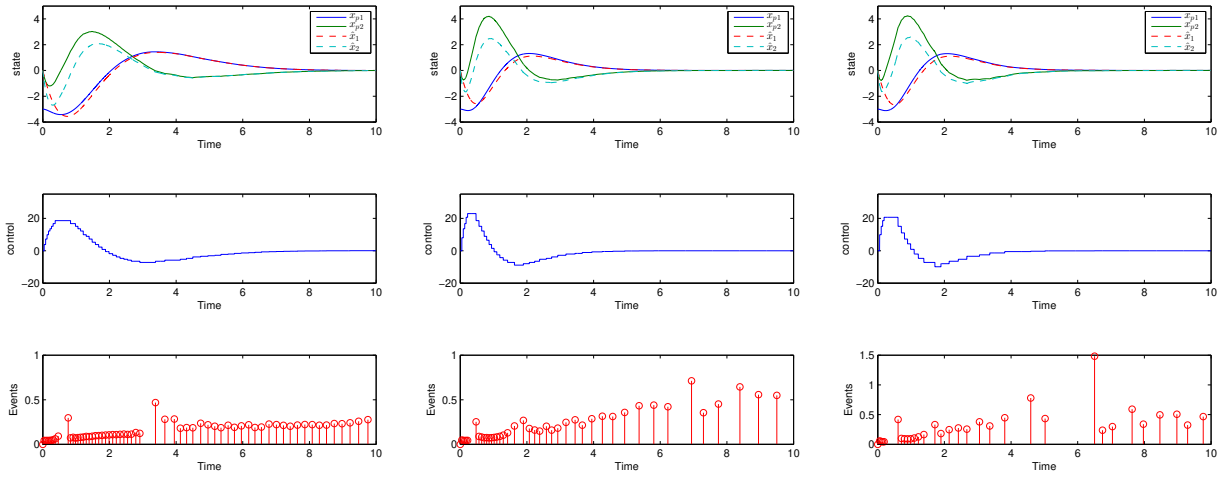

a) Emulation b) Co-design c) Co-design refinement

Figure 4: Example 1 – Evolution of the state of the plant and the observer, the control input u, and the sampling instants. $T = 0.043$

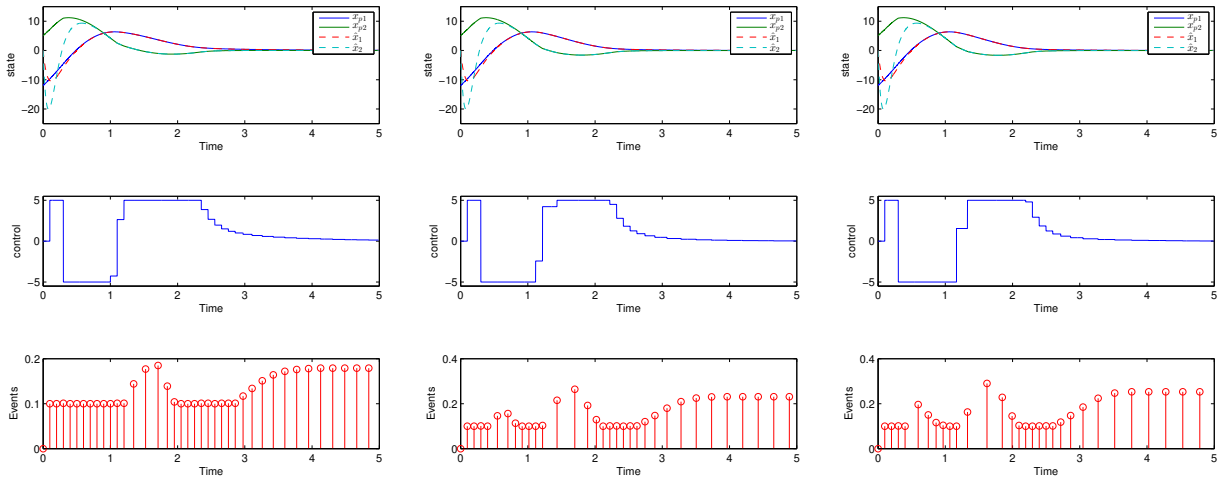

a) Emulation b) Co-design c) Co-design refinement

Figure 5: Example 2 – Evolution of the state of the plant and the observer, the control input u, and the sampling instants. $T = 0.1$

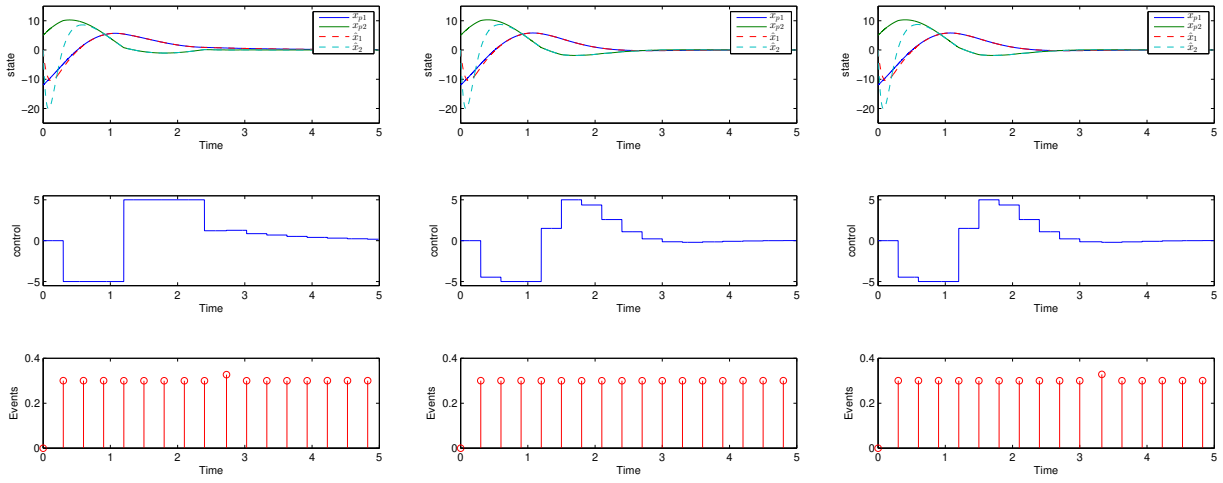

a) Emulation b) Co-design c) Co-design refinement

Figure 6: Example 2 – Evolution of the state of the plant and the observer, the control input u, and the sampling instants. $T = 0.3$